

MULTI-FREQUENCY PASSIVE NONLINEAR TARGETED ENERGY TRANSFERS IN SYSTEMS OF COUPLED OSCILLATORS

Stylianos Tsakirtzis ⁽¹⁾, Panagiotis N. Panagopoulos ⁽¹⁾, Gaetan Kerschen ⁽²⁾,
Oleg Gendelman ⁽³⁾, Alexander F. Vakakis ^(4,†), Lawrence A. Bergman ⁽⁵⁾

⁽¹⁾ School of Applied Mathematical and Physical Sciences,
National Technical University of Athens,

tsakstel@central.ntua.gr, panago58@central.ntua.gr

⁽²⁾ Département d'Aérospatiale, Mécanique et Matériaux (ASMA),
Université de Liège, g.kerschen@ulg.ac.be;

currently, postdoctoral fellow, National Technical University of Athens
and University of Illinois at Urbana – Champaign

⁽³⁾ Faculty of Mechanical Engineering,

Technion – Israel Institute of Technology, ovgend@techunix.technion.ac.il

⁽⁴⁾ School of Applied Mathematical and Physical Sciences,

National Technical University of Athens, vakakis@central.ntua.gr;

and

Department of Mechanical and Industrial Engineering (adjunct),

Department of Aerospace Engineering (adjunct),

University of Illinois at Urbana-Champaign, avakakis@uiuc.edu

⁽⁵⁾ Department of Aerospace Engineering,

University of Illinois at Urbana-Champaign, lbergman@uiuc.edu

Keywords: Nonlinear coupled oscillators, passive energy transfer

Abstract. *We study the dynamics of a system of coupled linear oscillators with a multi-DOF end attachment with essential (nonlinearizable) stiffness nonlinearities. We show numerically that the multi-DOF attachment with damping can passively absorb broadband energy from the linear system in a one-way, irreversible fashion, acting in essence as nonlinear energy sink (NES). Strong passive targeted energy transfer from the linear to the nonlinear subsystem is possible, over wide frequency and energy ranges. We numerically demonstrate that the topological structure of the periodic orbits in the frequency – energy plane of the underlying hamiltonian system greatly influences the strength of targeted energy transfer in the damped system, and governs to a great extent the overall transient damped dynamics. This work may be regarded as a contribution towards proving the efficacy the utilizing essentially nonlinear attachments as passive broadband boundary controllers.*

1 INTRODUCTION

We study the dynamics of a two-degree-of-freedom (DOF) linear system coupled to a multi-DOF essentially nonlinear attachment. Interesting energy exchange phenomena can occur in this type of coupled oscillators, including numerous coexisting branches of subharmonic periodic solutions, and one-way, irreversible transfer of energy from the linear oscillator to the nonlinear attachment, termed *targeted nonlinear energy pumping*. Such energy exchanges are often associated with transient or sustained *resonance captures* [1,2], whereby the nonlinearizable, nonlinear attachment engages in transient resonance with the linear oscillator, before the dynamics ‘escape’ to a different regime of the motion. In cases where the nonlinear attachment acts as passive recipient of vibration energy from the linear oscillator, it essentially acts as *nonlinear energy sink (NES)*.

In this work we show that multi-DOF NESs are capable of passively absorbing broadband energy from the primary linear systems to which they are attached. Moreover, this targeted energy transfer is more profound compared to analogous transfers in single-DOF NESs. Alternative configurations of single-DOF NESs were considered in previous works [3,4], whereas alternative mechanisms of targeted energy transfer were studied by other authors [5-8].

2 NUMERICAL EVIDENCE OF PASSIVE ENERGY TRANSFER

The system considered is depicted in Figure 1. It consists of a two-degree-of-freedom (DOF) linear primary oscillator connected through a weak linear stiffness of constant ε (which is the small parameter of the problem,

$0 < \varepsilon \ll 1$) to a three-DOF nonlinear attachment possessing essential stiffness nonlinearities. Each mass of the primary system is normalized to unity, and the stiffnesses of the nonlinear attachment obey cubic laws with constants C_1 and C_2 , and have no linear terms; thus they are essentially nonlinear (nonlinearizable); each mass of the nonlinear attachment is equal to μ , and both linear and nonlinear subsystems possess linear viscous dampers with small constants $\varepsilon\lambda$. Assuming that impulsive excitations $F_1(t)$ and $F_2(t)$ are applied to the primary system no direct forcing excites the nonlinear attachment, the equations of motion are,

$$\begin{aligned} \ddot{u}_1 + (\omega_0^2 + \alpha)u_1 - \alpha u_2 + \varepsilon\lambda\dot{u}_1 &= F_1(t) \\ \ddot{u}_2 + (\omega_0^2 + \alpha + \varepsilon)u_2 - \alpha u_1 - \varepsilon v_1 + \varepsilon\lambda\dot{u}_2 &= F_2(t) \\ \mu\ddot{v}_1 + C_1(v_1 - v_2)^3 + \varepsilon(v_1 - u_2) + \varepsilon\lambda(\dot{v}_1 - \dot{v}_2) &= 0 \\ \mu\ddot{v}_2 + C_1(v_2 - v_1)^3 + C_2(v_2 - v_3)^3 + \varepsilon\lambda(2\dot{v}_2 - \dot{v}_1 - \dot{v}_3) &= 0 \\ \mu\ddot{v}_3 + C_2(v_3 - v_2)^3 + \varepsilon\lambda(\dot{v}_3 - \dot{v}_2) &= 0 \end{aligned} \quad (1)$$

In the limit $\varepsilon \rightarrow 0$ the system decomposes into two uncoupled oscillators: a two-DOF linear primary system with natural frequencies $\omega_1 = \sqrt{\omega_0^2 + 2\alpha}$ and $\omega_2 = \omega_0 < \omega_1$, corresponding to out-of-phase and in-phase linear modes, respectively; and a three-DOF essentially nonlinear oscillator with a rigid body mode, and two flexible nonlinear normal modes – NNMs.

The aim of this work is to study the dynamics of this system, and to show that it is possible to achieve passive and irreversible *targeted energy transfer (energy pumping)* from the directly forced primary system to the nonlinear attachment; in that context, the nonlinear attachment will act as *nonlinear energy sink (NES)*. This work differs from previous works on targeted energy transfer in two basic aspects: first, it considers the possibility of *multi-frequency targeted energy transfer* from multiple modes of the primary system to multiple (nonlinear) modes of the NES; in addition, it shows that complex transitions in the damped dynamics can be related to the topological structure of the periodic orbits of the corresponding undamped system.

The study of the damped dynamics is performed initially through direct numerical simulations of the equations of motion and post processing of the transient results. An extensive series of numerical simulations was performed over different regions of the parameter space of the system, in order to establish the system parameters for which optimal passive energy transfer from the primary system to the NES occurs. Moreover, by varying the linear coupling stiffness α of the primary system we studied the influence of the closeness of the natural frequencies ω_1 and ω_2 of the two linear ('uncoupled') modes of the primary system on this targeted energy transfer. The numerical simulations were carried out by assigning different sets of initial conditions of the primary system, and always considering the NES to be initially at rest. To assess the degree of passive targeted energy transfer to the NES, the following energy measure was numerically computed,

$$E(t) = \frac{\varepsilon\lambda}{E_{in}} \int_0^t \left[(\dot{v}_1(\tau) - \dot{v}_2(\tau))^2 + (\dot{v}_2(\tau) - \dot{v}_3(\tau))^2 \right] d\tau \quad (2)$$

where E_{in} is the input energy provided to the system by the initial conditions. This nondimensional energy measure represents the instantaneous portion of input energy dissipated by the NES up to time instant t . Clearly, for transient excitation of the passive system (1) this instantaneous energy measure is expected to reach a definite asymptotic limit:

$$E_{NES} = \lim_{t \rightarrow \infty} E(t) \quad (3)$$

This asymptotic energy measure represents the portion of input energy *eventually* dissipated by the NES. In what follows, we use the asymptotic evaluation (3) as a measure of the efficiency of targeted energy transfer from the primary system to the NES.

The numerical simulations indicated that, for small values of the perturbation parameter ε , *enhanced passive targeted energy transfer from the primary system to the NES could be achieved for small values of the mass parameter μ and nonlinear characteristic C_2 of the NES, with all other parameters being quantities of $O(1)$* . This combination of system parameters led to large relative internal displacements in the NES, which, in turn, produced large values of the dissipated energy measures (2) and (3). Accordingly, in the following numerical simulations the system parameters were assigned the values:

$$\varepsilon = 0.2, \alpha = 1.0, C_1 = 4.0, C_2 = 0.05, \varepsilon\lambda = 0.01, \mu \rightarrow \varepsilon^2\mu = 0.08, \omega_0^2 = 1.0$$

The results presented in this work demonstrate the potential of system (1) to passively channel energy from the directly excited primary system to the nonlinear attachment, in a one-way, irreversible fashion.

In the following numerical simulations three types of impulsive forcing conditions - IFCs (or, equivalently, initial conditions) for the primary system are considered:

II: Single impulse forcing, $F_1(t) = Y\delta(t)$ (or, equivalently, $\dot{u}_1(0) = Y$), and all other initial

conditions zero.

I2: In-phase impulsive forcing, $F_1(t) = F_2(t) = Y\delta(t)$ and all other initial conditions zero.

I3: Out-of-phase impulsive forcing, $F_1(t) = -F_2(t) = Y\delta(t)$ and all other initial conditions zero.

In Figures 2-4 we depict the energy measure E_{NES} as function of the magnitude of the impulse Y and the linear coupling stiffness of the primary system α , for the above types of IFCs. The following conclusions are drawn from these results.

In all cases, a significant portion (reaching as high as 86% for IFC I1; 92% for IFC I2; and 90% for IFC I3) of the input energy gets passively absorbed and dissipated by the NES. This significant passive targeted energy transfer occurs in spite of the fact that the (directly forced) primary linear system and the NES have identical dashpots. Moreover, the energy transfer is *broadband*.

Whereas the portion of energy eventually dissipated at the NES, E_{NES} , depends on the level of energy input and the closeness of the natural frequencies of the primary system, this dependence is less pronounced compared to single-DOF NES. This is concluded by comparing the plots of Figures 2-4 with results reported in earlier works where grounded single-DOF NESs were considered [4]. The enhanced targeted energy transfer achieved through the use of multi-DOF NESs is concluded from the comparative plots of Figure 5, where the energy measure E_{NES} is depicted for a system with $\alpha = 0.2$, and IFCs I1 and I3. The system with single-DOF NES whose response is depicted in that plot is identical to that of Figure 1, but with the multi-NES replaced by a single mass $3\epsilon\mu$ grounded by means of a cubic stiffness nonlinearity with characteristic Cv^3 , $C = 1.0$, and a weak viscous damper $\epsilon\lambda$. We note the significant improvement of targeted energy transfer achieved by using the multi-DOF NES, and the less pronounced dependence on the magnitude of the input impulse Y in that case.

Particularly notable is the capacity of the multi-DOF NES to absorb a significant portion of the input energy even at low values of the applied impulse. Such low-energy targeted energy transfer is markedly different from the performance of single-DOF NESs, which, as reported in previous works [4,8], is ‘activated’ only when the magnitude of input energy exceeds a certain critical threshold; for the case of multi-DOF NES such a critical energy threshold can only be detected in the energy plot for $\alpha = 4$ of Figure 4, i.e., only in the case when the primary system possesses well separated natural frequencies and is excited through out-of-phase initial conditions. In all other cases (Figures 2-4) no such critical input energy threshold is identified, for the multi-DOF NES. This interesting feature of the dynamics will be reconsidered in more detail in a later section.

Of particular interest is the plot of E_{NES} in Figure 4 corresponding to $\alpha = 1$ (corresponding to natural frequencies of the uncoupled primary system $\omega_1 = 1.7321$, $\omega_2 = 1.0$ rad/sec) and out-of-phase impulse excitations. For small impulse magnitudes, the portion of energy dissipated at the NES develops a local minimum before reaching higher values. To get some insight into the dynamics of targeted energy transfer in that region, in Figures 6 and 7 we depict the numerical Cauchy wavelet transforms (WTs) of the internal relative NES displacements $[v_2(t) - v_1(t)]$ and $[v_3(t) - v_2(t)]$ at points labeled A and B in Figure 4; point A is a case where no rigorous energy transfer to the NES, in contrast to point B where nearly 90% of the input energy gets absorbed and dissipated by the NES. The WT can be viewed as a basis for functional representation but is at the same time a relevant technique for time-frequency analysis. In contrast to the Fast Fourier Transform (FFT) which assumes signal stationarity, the WT involves a windowing technique with variable-sized regions. Small time intervals are considered for high frequency components whereas the size of the interval is increased for lower frequency components, thereby giving better time and frequency resolutions than the FFT. The plots shown represent the amplitude of the WT as a function of frequency (vertical axis) and time (horizontal axis). Heavy shaded areas correspond to regions where the amplitude of the WT is high whereas lightly shaded regions correspond to low amplitudes. Such plots enable one to deduce the temporal evolutions of the dominant frequency components of the signals analyzed. Comparing the two responses of Figures 6 (point A) and 7 (point B), it is clear that the enhanced energy transfer in the later case is due mainly to the large-amplitude transient relative response $[v_3(t) - v_2(t)]$; judging from the corresponding WT, this time series consists of a ‘fast’ oscillation with frequency close to ω_1 , modulated by a large-amplitude ‘slow’ modulation. Moreover, this modulated response is not sustained over all times; rather, it takes place only at the initial phase of the motion, and escapes this regime of the motion at approximately $t = 50$. Similar behavior is observed for the time series of the other relative response, $[v_2(t) - v_1(t)]$, in Figure 7. It is well established [4,13,14] that this represents a *transient resonance capture (TRC)* of the NES dynamics on a resonance manifold near the out-of-phase linear mode of the uncoupled primary system, which results in enhanced and irreversible energy transfer from the primary system to the NES. Comparing to the responses of Figure 6 (where less significant energy transfer occurs), we note that the transient responses are dominated by sustained frequency components, indicating excitation of nonlinear modes, rather than occurrence of TRCs; the frequencies of some of the nonlinear modes

that are excited differ from the linearized natural frequencies ω_1 and ω_2 , indicating the presence in the response of essentially nonlinear modes with no linear analogs.

3 DAMPED TRANSITIONS IN THE FREQUENCY – ENERGY PLANE

We wish to study in more detail the damped transitions associated with the peculiar behavior of the targeted energy transfer plot for $\alpha = 1.0$ and impulsive forcing conditions I3 (depicted in Figure 4). More specifically, it was numerically found that when the linear system is excited by a pair of anti-phase impulses of magnitude Y , strong targeted energy transfer to the NES occurs at low values of the impulse (as much as 90% for $Y=0.1$); for increasing magnitude of the impulse the eventual energy transfer to the NES first decreases (reaching nearly 50% for $Y=1.0$), before increasing again to high levels (up to nearly 90% for $Y=1.5$). Further increase of Y decreases the portion of input energy that is eventually dissipated at the NES. The damped transitions leading to this peculiar behavior of the energy transfer capacity of the NES are depicted and analyzed in Figures 8-10. We will superimpose the wavelet transforms of the NES relative displacements to the frequency energy plot of the periodic orbits of the underlying hamiltonian system with no damping (these were computed in [15]).

In Figure 8 the damped response of the system is depicted for impulsive forcing conditions I3 and $Y=0.1$ (i.e., impulses $F_1(t) = -F_2(t) = Y\delta(t)$ and zero ICs). In this case both internal NES displacements $[v_1(t) - v_2(t)]$ and $[v_2(t) - v_3(t)]$ follow regular backbone branches. The relative displacement $[v_1(t) - v_2(t)]$ has a dominant frequency component that approaches a linearized natural frequency with decreasing energy; by contrast, $[v_2(t) - v_3(t)]$ has two strong harmonic components that approach two other linearized natural frequencies for decreasing energy, indicating *multi-frequency transfer of energy simultaneously from two modes of the linear limiting system* (5). Moreover, the same backbone branches are tracked by the response throughout the motion, and strong energy transfer occurs right from the early stage of the response. This explains the strong eventual energy transfer to the NES (~90%) that occurs for this low impulse excitation.

By increasing the magnitude of the impulse to $Y=1.0$ the overall energy transfer from the linear to the nonlinear subsystem significantly decreases. The damped response in this case is depicted in Figure 9, where some major qualitative differences are observed compared to the previous simulation. Judging from the partition of the instantaneous energy among the linear and nonlinear subsystems, it is concluded that in the energy transfer is significantly delayed, which explains the weak eventual energy transfer to the NES (~50%). This delay is explained when one studies the wavelet transforms of the NES responses in the frequency – energy plot of Figure 9a. At the initial stage of the motion there occurs strong resonance capture of the damped motion by the out-of-phase mode of the linear subsystem; this results in a motion mainly localized to the (directly excited) linear subsystem, with a small portion of energy ‘spreading out’ to the NES. As energy decreases due to damping dissipation, the damped motion ‘escapes’ from out-of-phase resonance capture, and follows regular backbone branches; this results in strong energy transfer develops (as in the simulations of Figure 8), which, however, is delayed at a stage where the overall level of energy of the system is already small. Hence, no significant overall targeted energy transfer from the linear subsystem to the NES occurs in this case.

Increasing the magnitude of the impulse to $Y=1.5$ enables the system to escape from the strong initial out-of-phase resonance capture, leading to resumed strong targeted energy transfer. This is depicted in Figure 10, showing that the NES relative responses possess multiple strong frequency components, indicating that strong targeted energy transfer occurs at multiple frequencies. Note in this case the early strong energy transfer from the linear subsystem to the NES that results in an eventual targeted energy transfer of nearly 90%.

4 CONCLUDING REMARKS

The dynamical system considered in this work possesses complicated dynamics due to its degenerate structure. The system has strong passive targeted energy transfer capacity, leading, in some cases, to as much as 90% of input energy in the linear subsystem being irreversibly transferred to, and dissipated at the nonlinear attachment; then the attachment acts in essence as nonlinear energy sink. The capacity of the attachment to irreversibly absorb broadband vibration energy was demonstrated numerically in this work, but it can also be analytically studied by reduction and local slow/fast partition of the damped dynamics. It was shown that multi-DOF essentially nonlinear attachments may be more efficient energy absorbers than single-DOF ones, since they are capable of absorbing energy simultaneously from multiple modes of the linear subsystem, and over wider frequency and energy ranges. Passive targeted energy transfer can be related to transient resonance captures (TRCs) in the damped dynamics, whereby orbits of the system in phase space are captured transiently in neighborhoods of resonance manifolds.

ACKNOWLEDGMENTS

This work was supported in part by a grant for basic research ‘HRAKLEITOS’ funded by the European

Commission and the General Secretariat for Research and Technology, Hellenic Ministry of Development; by AFOSR grant FA9550-04-1-0073; by the Taub and Shalom Foundations (Horev fellowship); and by grants from the Belgian National Fund for Scientific Research - FNRS, the Belgian Rotary District 1630, and the Fulbright and Duesberg Foundations.

REFERENCES

- [1] Arnold V.I. (ed.), 1988, *Dynamical Systems III*, Encyclopaedia of Mathematical Sciences, Springer Verlag, Berlin and New York.
- [2] Quinn, D., 1997, 'Resonance Capture in a Three Degree of Freedom Mechanical System,' *Nonlinear Dynamics* 14, 309-333.
- [3] Vakakis A.F., Gendelman O., 2001, 'Energy Pumping in Nonlinear Mechanical Oscillators II: Resonance Capture,' *Journal of Applied Mechanics* 68(1), 42-48.
- [4] Vakakis A.F., McFarland D.M., Bergman L.A., Manevitch L.I., Gendelman O., 2004, 'Isolated Resonance Captures and Resonance Capture Cascades Leading to Single- or Multi-Mode Passive Energy Pumping in Damped Coupled Oscillators,' *Journal of Vibration and Acoustics*, 126 (2), 235-244.
- [5] Kopidakis G., Aubry S., Tsironis G.P., 2001, 'Targeted Energy Transfer Through Discrete Breathers in Nonlinear Systems,' *Physical Review Letters*, 87 (16), paper 165501-1.
- [6] Aubry S., Kopidakis S., Morgante A.M., Tsironis G.P., 2001, 'Analytic Conditions for Targeted Energy Transfer Between Nonlinear Oscillators or Discrete Breathers,' *Physica B* 296, 222-236.
- [7] Gendelman O.V., Vakakis A.F., Manevitch L.I. and McCloskey R., 2001, 'Energy Pumping in Nonlinear Mechanical Oscillators I: Dynamics of the Underlying Hamiltonian System,' *Journal of Applied Mechanics* 68(1), 34-41.
- [8] Panagopoulos P.N., Vakakis A.F., Tsakirtzis S., 2004, 'Transient Resonant Interactions of Linear Chains with Essentially Nonlinear End Attachments Leading to Passive Energy Pumping,' *International Journal of Solids and Structures*, 41 (22-23), 6505-6528.
- [9] S. Tsakirtzis, P.N. Panagopoulos, G. Kerschen, O. Gendelman, A.F. Vakakis, L.A. Bergman, 2005, 'Complex Dynamics and Targeted Energy Transfer in Systems of Linear Oscillators Coupled to Multi-degree-of-freedom Essentially Nonlinear Attachments,' *Physical Review E* (submitted).

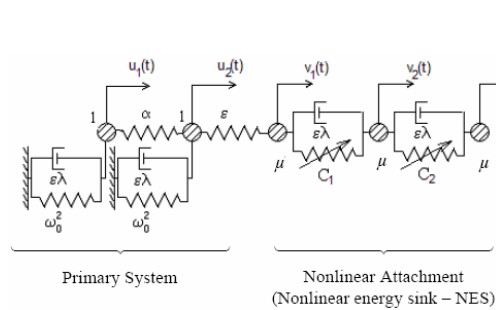


Figure 1. Primary (linear) system with multi-degree-of-freedom (MDOF) nonlinear attachment

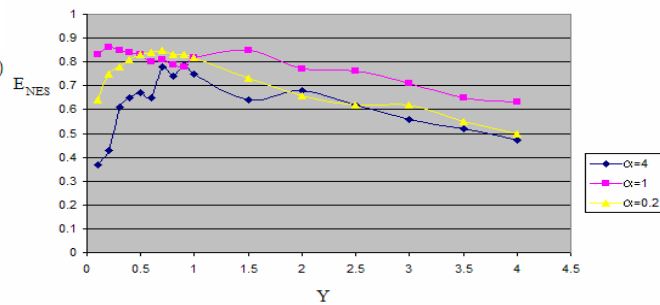


Figure 2. Portion of energy eventually dissipated at the nes for varying values of single impulse Y (impulsive forcing condition I1), and coupling stiffness α of the primary system

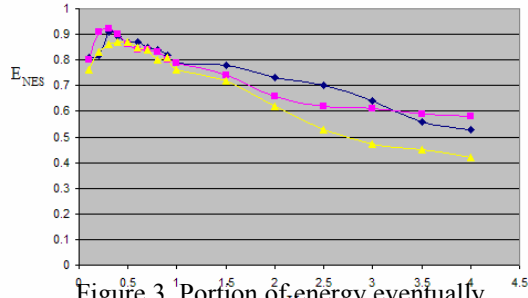


Figure 3. Portion of energy eventually dissipated at the nes for varying values of single impulse Y (impulsive forcing condition I2), and coupling stiffness α of the primary system

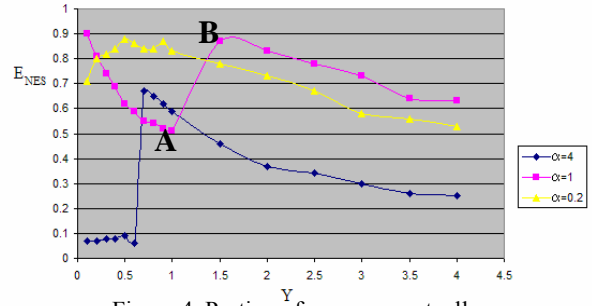


Figure 4. Portion of energy eventually dissipated at the nes for varying values of single impulse Y (impulsive forcing condition I3), and coupling stiffness α of the primary system; the letters A and B at the plot for $\alpha = 1$ refer to the results depicted in figures 6 and 7.

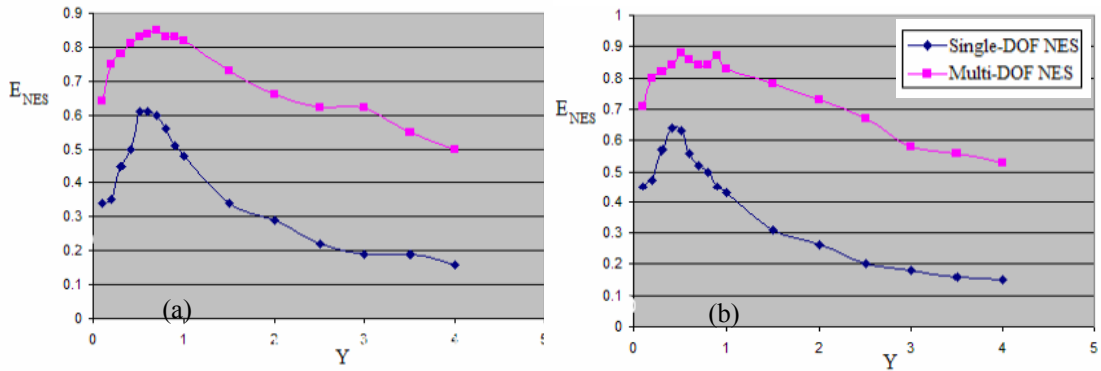


Figure 5. Energy measures E_{NES} for primary systems with single- and multi-DOF NESs, and impulsive forcing conditions, (a) I1, and (b) I3

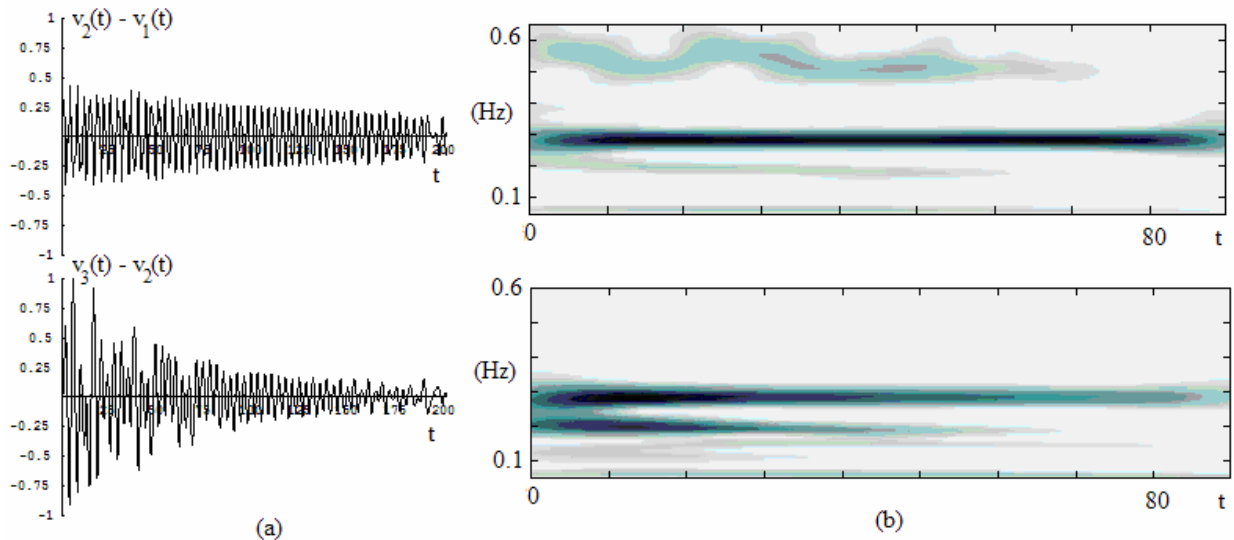


Figure 6. Internal NES relative displacements for out-of-phase impulses (I3) with $Y=1$ and $\alpha=1$ (point A in figure 4): (a) time series, (b) Cauchy wavelet transforms

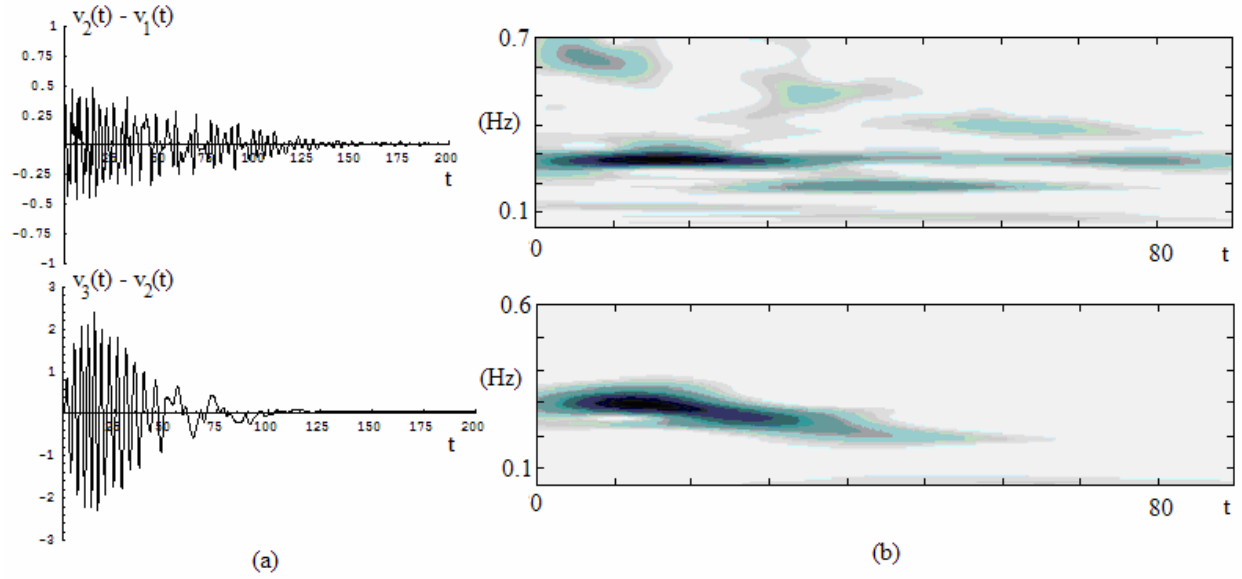


Figure 7: Internal NES relative displacements for out-of-phase impulses (I3) with $Y=1.5$ and $\alpha=1$ (point B in figure 4): (a) time series, (b) Cauchy wavelet transforms

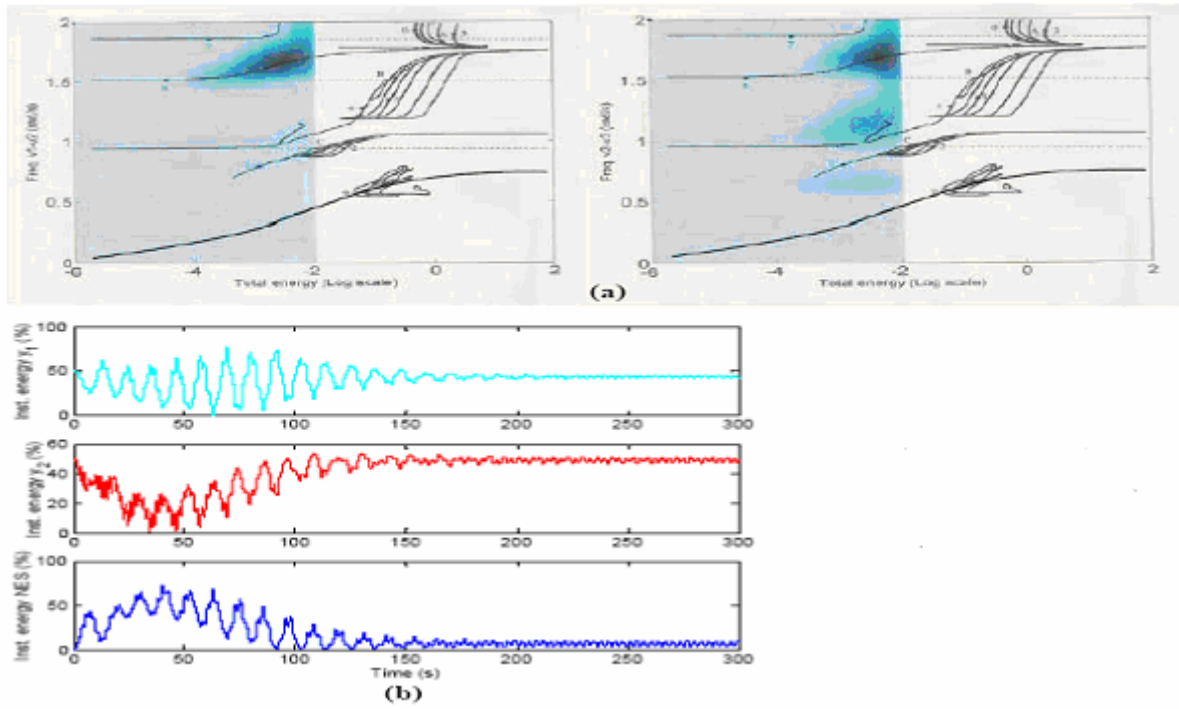


Figure 8: Damped responses for out-of-phase impulses $Y=0.1$ (impulsive forcing condition I3); (a) Cauchy wavelet transforms superimposed to the frequency – energy plot of the periodic orbits of the underlying hamiltonian system [9], (b) partition of instantaneous energy of the system.

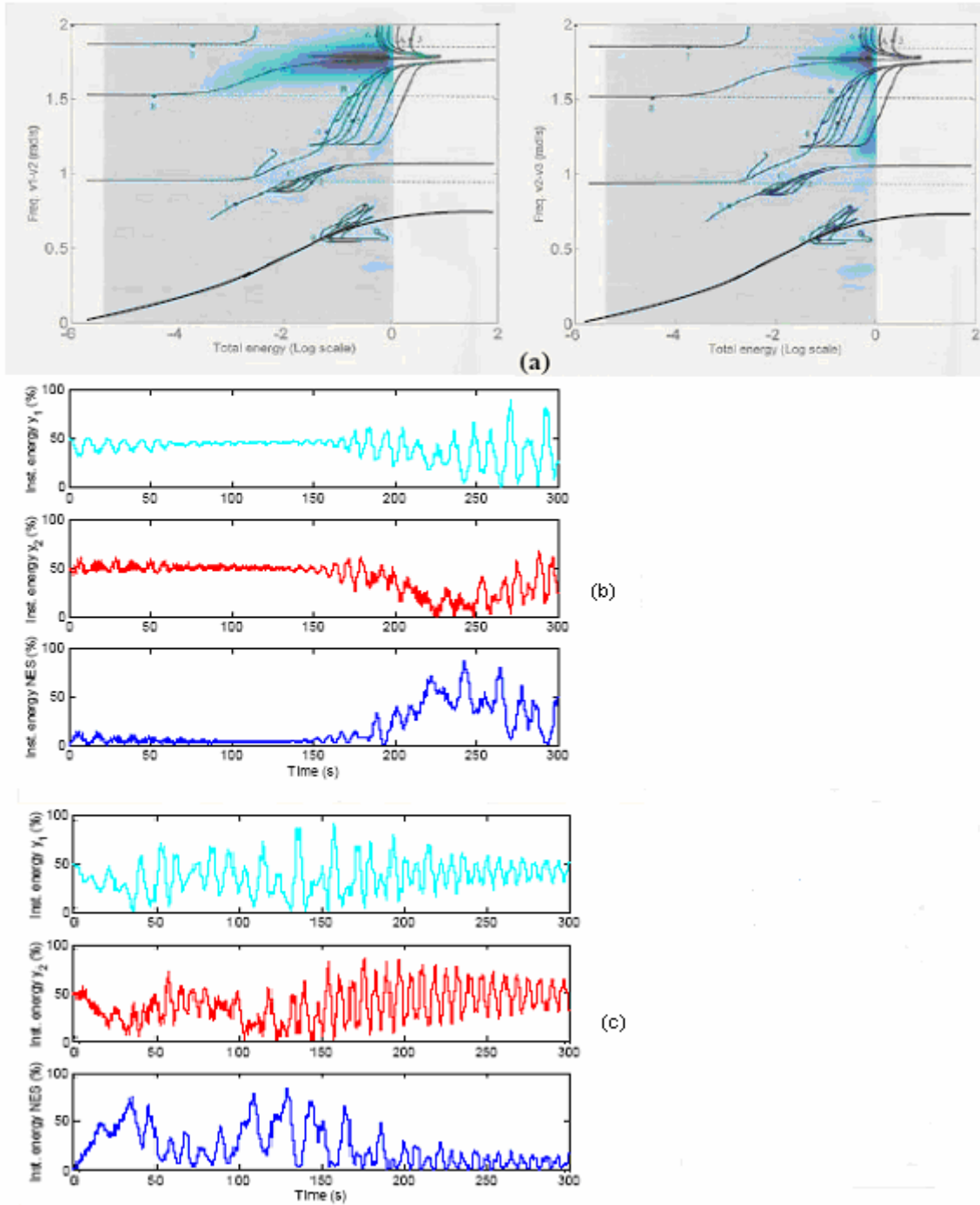


Figure 9: (a) Cauchy wavelet transforms superimposed to the frequency – energy plot of the periodic orbits of the underlying hamiltonian system [9], (b) Damped responses for out-of-phase impulses $Y=1.0$ (impulsive forcing condition I3partition of instantaneous energy of the system, (c) Damped responses for out-of-phase impulses $Y=1.5$ (impulsive forcing condition I3partition of instantaneous energy of the system